Effect of SBS molecular structure on the rheological properties of ternary nanomodified bituminous binders

Effect of SBS molecular structure on the rheological properties of ternary nanomodified bituminous binders

Abstract: The work presented in this paper focused on the rheological properties of ternary composites for paving applications constituted by bitumen, nano-sized additives and polymer modifiers. Non-functionalized multiwall carbon nanotubes and two types of styrene-butadiene-styrene polymers, linear and radial, were used to modify a reference neat bitumen with the specific goal of highlighting the effects of polymer structure on the final properties of composites. Binary blends containing a single additive were also investigated for comparative purposes. Materials were characterized by means of dynamic mechanical analysis and their internal structure was assessed with fluorescence microscopy observations. Experimental outcomes indicated that polymer architecture played a crucial role in promoting effective interactions between modifiers and carbon nanotubes. Specifically, in the presence of linear styrene-butadiene-styrene, carbon nanotubes acted as compatibility activators, leading to the formation of stable and continuous ternary systems. On the contrary, in the case of radial styrene-butadiene-styrene, beneficial effects provided by nano-modification were jeopardized by the increased thermodynamic instability which resulted from the combined use of these two components.

Keywords: bituminous binders; styrene-butadiene-styrene; carbon nanotubes; molecular structure; rheology

1 INTRODUCTION

The use of thermoplastic polymers for the modification of bitumen has seen a widespread diffusion in the road paving industry over the past decades. In fact, it has been proven that polymer-modified bituminous binders can significantly contribute to prevent the main distress phenomena typically affecting flexible pavements, thus ensuring increased service lives and reducing costs related to maintenance and rehabilitation operations [1].

Among the various types of polymers usually employed for bitumen modification, styrene-butadiene-styrene (SBS) elastomers are by far the most popular. These polymers are characterized by a biphasic structure composed of rigid domains of styrene connected to a soft matrix of butadiene molecules which provides the material with pronounced elastic properties. When mixed with bitumen at high temperatures, SBS is partially swollen by the lighter fractions of maltenes, that constitute with asphaltenes the colloidal structure of bitumen. This interaction leads to the consequent creation of polymer-rich and asphaltene-rich phases which coexist in metastable equilibrium [2]. Final properties of polymer-modified binders are largely dependent upon the morphological configuration of this two-phase system [3-5].

More recently, scientific pursuits have started moving towards the use of alternative solutions for binder modification based on the implementation of nano-technologies. The idea of a selective modification of bitumen at the nano-scale may open new scenarios in the development of advanced materials with properties tailored to suit specific needs, such as the capability of withstanding extreme environmental and loading conditions caused by climatic changes as well as increasing traffic loads [6-7]. In this context, carbon nanotubes (CNTs) are considered the most promising products due to their unique mechanical properties and to their large surface area-to-volume ratio [8-10]. CNTs are one-dimensional carbon materials which consist of graphene sheets of sp^2-hybridized carbon atoms rolled up into cylindrical structures of nanometric diameter. Depending upon the number of coaxial tubular shells of which they are composed, they can be found in either single-wall or multiwall configurations [11].

Moving from the idea of synergistically combining the beneficial effects provided by nano-reinforcing agents and polymeric modifiers, some pioneering research works on ternary SBS/CNT/bitumen composites have been carried out in the last few years. Wang et al. [12] examined the role played by functionalized multiwall CNTs in the micromorphology of polymer-modified bitumens. The authors highlighted that CNTs strengthen the interfacial interactions which arise between linear SBS and bitumen, thereby affecting the swelling mechanism of the polymer-rich phase. Goli et al. [13] focused on the influence of CNTs on the storage stability of polymer-bitumen blends. They reported that nano-particles improved the stability of SBS-modified binders, indicating an efficient interaction with base components. Wang et al. [14] analysed the overall

performance properties of ternary bituminous systems containing functionalized multiwall CNTs and linear SBS. Experimental results showed that the major benefits yielded by CNTs are the enhancement of anti-ageing properties and of resistance to permanent deformation and fatigue cracking. Shu et al. [15] investigated the performance of bituminous binders modified with linear SBS and multiwall CNTs. They found that in addition to a better thermal stability, the presence of CNTs led to an overall improvement of performance in high- and low-temperature conditions.

The research work described in this paper aims at increasing current knowledge about nanocomposites for paving applications by providing new insights into the interactions between polymer modifiers and nano-sized additives. Specifically, the performed investigation focused on the effects of polymer molecular structure (linear or radial) on the rheological properties of ternary bituminous-based nanocomposites. Rheological characterization was carried out via Dynamic Mechanical Analysis (DMA) in a wide range of temperatures and loading frequencies. In order to link rheological data to internal structure, nanocomposites were also subjected to a direct morphological analysis by means of fluorescence microscopy.

2 BASE MATERIALS AND BLEND PREPARATION

Ternary nanocomposites considered in the investigation were obtained by combining one base bitumen, one type of non-functionalized multiwall CNTs and two types of SBS block copolymers.

The base binder was a 70/100 penetration grade bitumen characterized by a softening point of 44.6 ℃ (EN1427) and a penetration at 25 ℃ of 95.4 dmm (EN 1426). As per AASHTO M320, this binder was subjected to performance grading tests. The corresponding results, which indicated that the bitumen is of Performance Grade (PG) PG58-22, are summarized in Table 1.

A chemical portrayal of the bitumen was carried out by means of a solubility-based analysis which leads to the assessment of the relative amounts of saturates, aromatics, resins and asphaltenes. The four fractions were separated on silica rods via a thin layer chromatography and quantified by means of a flame ionization detection device [16-17]. A typical output of such an analysis is presented in Figure 1 in the form of a chromatogram, in which the electrical potential difference ΔV recorded during the flame ionization phase is plotted as a function of rod burning time. Figure 1 also displays the average percentages of the four fractions obtained from a set of ten rods.

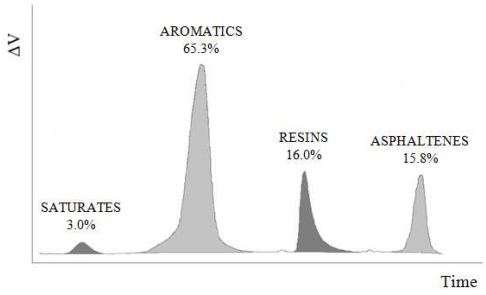

Figure 1 Chromatogram of base bitumen.

Table 1 Performance grading test results (base bitumen).

Ageing condition	PG parameter	Measured value
Original	T = 135 ℃	η = 0.347 Pa·s
	|G*|/sinδ = 1 kPa	T = 63.3 ℃
RTFO	|G*|/sinδ = 2.2 kPa	T = 63.8 ℃
	|G*|·sinδ = 5000 kPa	T = 22.0 ℃
PAV	m = 0.300	T = -14.3 ℃
	S = 300 MPa	T = -16.2 ℃

RTFO: Rolling Thin Film Oven (short-term ageing); PAV: Pressure Ageing Vessel (long-term ageing);

η: dynamic viscosity (Brookfield viscometer); T: test temperature; |G*| and δ: norm and phase angle of the complex modulus (Dynamic Shear Rheometer); m and S: creep rate and creep stiffness (Bending Beam Rheometer).

The CNTs employed in the investigation were commercially available products manufactured by means of the chemical vapour deposition process. They are characterized by a non-functionalized multiwall structure which guarantees an aspect ratio greater than 150 with limited production costs. Main characteristics of the employed CNTs, based on the manufacturer's technical specifications, are reported in Table 2.

The two types of SBS block copolymers, differing in molecular structure (radial branching and linear), were obtained by anionic polymerization, with the addition of a non-staining antioxidant system during production. They were specifically selected in order to have similar features in terms of physical and mechanical properties, with the purpose of highlighting the role played by the radial or linear molecular arrangement. Main characteristics of both modifiers are summarized in Table 3.

Table 2. Main characteristics of CNTs.

	Average diameter[1]	Average length[1]	Surface area[2]	Carbon purity[3]	Density
C (Carbon nanotubes)	9.5 nm	1.5 μm	250-300 m^2/g	90 %	1.72 g/cm^3

1: From transmission electron microscopy (TEM); 2: From Brunauer-Emmett-Teller analysis (BET); 3: From thermogravimetric analysis (TGA).

Table 3. Main characteristics of SBS polymers.

	Tensile strength[1]	Elongation at break[1]	Hardness[2]	Viscosity[3] (Toluene sol., 25 % wt)	Density[4]	Mass content of bound styrene
L (Linear SBS)	20 MPa	750 %	80 Sh A	4.0 Pa·s	0.94 g/cm^3	30 %
R (Radial SBS)	18 MPa	700 %	82 Sh A	20 Pa·s	0.94 g/cm^3	30 %

1: ASTM D 412; 2: ASTM D 2240; 3: ASTM D 1084; 4: ASTM D 412; 5: ASTM D 792.

Ternary blends composed of bitumen, SBS and CNTs were produced in the laboratory by using a fixed dosage for each additive. This was established on the basis of the results obtained from optimization processes developed in previous studies [18-20]. In order to thoroughly understand the effects of each component on ternary systems, viscoelastic properties of the abovementioned blends were compared to those of base bitumen and of binary composites containing a single additive type. Six different binders were thus considered in the experimental investigation, as displayed in Table 4.

Table 4. Binders considered in the investigation (dosages are expressed in percent by weight of base bitumen).

Blend code	Radial SBS	Linear SBS	Multiwall CNTs
B	0 %	0 %	0 %
BC	0 %	0 %	0.5 %
BR	3 %	0 %	0 %
BL	0 %	3 %	0 %
BRC	3 %	0 %	0.5 %
BLC	0 %	3 %	0.5 %

The protocol followed for the preparation of blends consists in a first phase of shear mixing followed by a second phase of sonication. Shear mixing was carried out at 180 ℃ by using a mechanical stirrer (Heid olph RZR 2041) equipped with a special disintegrating head made up of a ringed propeller-type impeller with shaft coupled to a fixed perforated plate. The shear mixing procedure begins with the preliminary homogenization

of additives into the preheated bitumen at low speed (500 rpm) for 2 minutes, after which speed is increased to 1550 rpm and kept constant for further 120 minutes. Based on previous studies focused on the beneficial effects of sonication in the production of bituminous nanocomposites [9], in the second phase of blend preparation ultrasounds are transmitted within the blend at a temperature of 150 ℃ with the use of an ultrasonic homogenizer (UP50H, Hielscher GmbH) equipped with a titanium sonotrode of 7 mm diameter. A wave of 158 μm amplitude is applied in the continuous mode at a frequency of 24 kHz for a total time of 60 minutes.

3 Dynamic Mechanical Analysis (DMA)

Rheological properties of the bituminous blends were determined by means of DMA using oscillatory tests, which led to the determination of the principal viscoelastic parameters. These included the norm ($|G^*|$) and the phase angle (δ) of the complex modulus, along with other derived parameters such as the storage (G') and loss (G'') moduli. Materials were subjected to frequency sweep tests covering two log-decades of angular frequency, from 1 rad/s to 100 rad/s, and a wide temperature range, from -36 ℃ to 82 ℃, with 6 ℃ increments between consecutive steps. Shear strains were varied depending upon the combination of temperature and frequency adopted for testing, thus allowing the rheological properties of the materials to be evaluated in their linear viscoelastic domain. The instrument used for measurements was a dynamic shear rheometer from Anton Paar Inc. (Physica MCR 302). Different testing geometries were adopted depending upon temperature interval, as follows: 25-mm parallel plates (PP25) with 1-mm gap between 40 ℃ and 82 ℃, 8-mm parallel plates (PP08) with 2-mm gap betwe en 4 ℃ and 34 ℃, 4-mm parallel plates (PP04) with 2-mm gap between -36 ℃ and 0 ℃. In order to avoid r uptures due to excessive thermal contraction forces, in this last temperature range the gap was reduced during conditioning by applying a normal force of 0.5 N. Moreover, relaxation phenomena were promoted by cooling the specimen according to predefined temperature gradients, thus avoiding a sudden temperature change between successive frequency sweeps.

4 Results

4.1 Raw data

Figure 2 shows a typical output of frequency sweep tests represented in the so-called Black space, which displays the norm versus the phase angle of the complex modulus. This type of representation portrays the overall rheological response of blends without any manipulations of raw data, thus allowing a preliminary analysis of the results, with the identification of possible rheological inconsistencies and the verification of the thermo-rheological simplicity of the materials. As expected, blends containing polymeric additives showed some “branching” and discontinuous “waves” in the Black plot, thus indicating a slight deviation with respect to target conditions in which the time-temperature equivalency is satisfied. Since such an evidence was limited to extreme temperature conditions (above 70 ℃), the time-temperature superposition principle was still considered to be valid for the subsequent analyses [21].

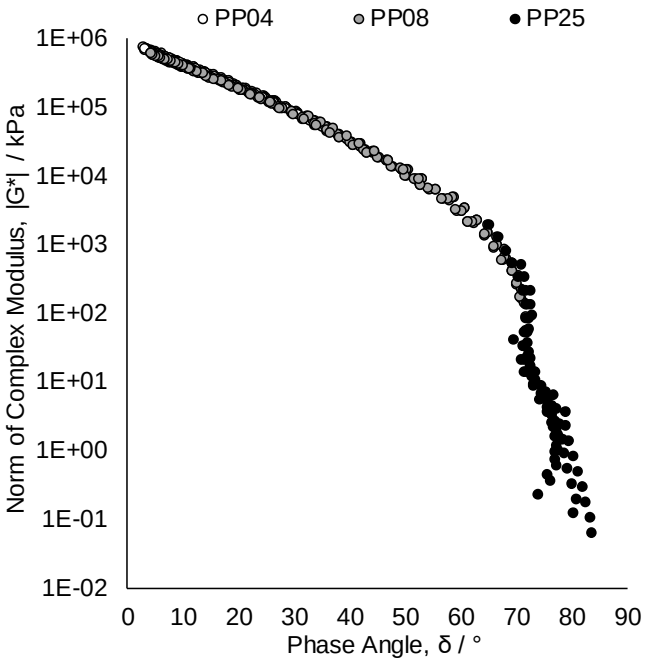

Figure 2. Example of Black plot (binder BR).

Preliminary analysis of raw data also involved evaluation of testing repeatability. For such a purpose, replicates carried out with a specific measuring device at the same temperature and angular frequency were used to determine repeatability values expressed in terms of the $d2s\%$ parameter. As indicated in Eq. 1, $d2s\%$ was calculated as the ratio between the absolute value of the difference in results $|\Delta X(T,\omega)|$ and their mean value $\overline{X(T,\omega)}$.

$$d2s\%\_X(T,\omega) = \frac{|\Delta X(T,\omega)|}{\overline{X(T,\omega)}} \cdot 100 \qquad \text{Eq. 1}$$

In order to provide a general overview of the repeatability for both the norm and the phase angle of the complex modulus, the mean value of $d2s\%$ was separately calculated for each measuring device and for each material. Corresponding results are summarized in Tables 5 and 6, respectively.

Table 5. Mean values of repeatability obtained for each measuring device.

	PP04 (-36 to 0) ℃	PP08 (4 to 34) ℃	PP25 (40 to 82) ℃
Mean $d2s\%\_\|G^*\|$ / %	3.8	7.1	7.1
Mean $d2s\%\_\delta$ / %	4.0	0.6	1.0

Table 6. Mean values of repeatability obtained for each material.

	B	BC	BL	BR	BLC	BRC
Mean $d2s\%\_\|G^*\|$ / %	2.7	12.1	5.5	3.4	2.6	7.5
Mean $d2s\%\_\delta$ / %	1.6	3.9	2.2	1.9	2.1	2.3

In general terms, it was observed that $|G^*|$ measurements were characterized (except in one case, discussed below) by a lower level of repeatability with respect to δ measurements, regardless of employed measuring device and tested material.

When focusing on the effects of measuring device, displayed data showed that the use of PP08 and PP25 resulted in very similar $d2s\%$ values. In comparison to those obtained with PP04, these values were significantly higher in the case of $|G^*|$ and significantly lower in the case of δ. This indicates that when operating at very low temperatures, at which tested materials were characterized by very high stiffness and pronounced elasticity, the equipment yielded a higher precision in imposing deflection angles counterbalanced by a lower precision in computing time shifts between applied torque and angular deformation.

When considering the effects related to the type of material, it was observed that the highest overall repeatability was obtained for base binder B, which was clearly the most homogeneous in nature. Conversely, repeatability was negatively affected by the addition of nano-sized or polymer modifiers, with the lowest level reached by binary blends containing CNTs. It is also interesting to notice that in the case of blends prepared with radial SBS, the presence of CNTs reduced repeatability as demonstrated by the higher $d2s\%$ value recorded for BRC as compared to that recorded for BR. On the contrary, in the case of blends containing linear SBS, a reduction in $d2s\%$ was found when passing from the binary to the ternary composite.

4.2 Shift factors

Analysis of rheological data involved the evaluation of temperature dependency, which provides information on the relaxation processes occurring within bitumen and on the interphase mechanisms taking place in blends [22]. For such a purpose, the analysis focused on the so-called shift factors, defined as the ratio of physical to reduced frequencies at a given reference temperature T_{ref}.

Shift factors of isotherm frequency sweeps were calculated according to the LCPC method, based on the Kramers-Kronig relations between the real and imaginary parts of a complex function [23]. This procedure has the main advantage of avoiding errors related to manual shifting operations without the need to link the shifting optimization to a specific fitting model.

The shift factor $a_{(T,T_{ref})}$of an isotherm obtained at the generic temperature T with respect to a reference temperature T_{ref} was calculated by means of Eq. 2-3:

$$log\left(a_{(T,T_{ref})}\right) = \sum_{j=1}^{j=ref} log\left(a_{(T_j,T_{j+1})}\right) \quad \text{Eq. 2}$$

$$log\left(a_{(T,T_{ref})}\right) = \sum_{j=1}^{j=ref} \frac{log\left(\left|G^*\left(T_j,\omega\right)\right|\right) - log\left(\left|G^*\left(T_{j+1},\omega\right)\right|\right)}{\delta_{avr}^{(T_j,T_{j+1})}(\omega)} \cdot \frac{\pi}{2} \quad \text{Eq. 3}$$

where $\delta_{avr}^{(T_j,T_{j+1})}$is the average of two phase angle values measured at T_j and T_{j+1} at angular frequency ω.

In Figure 3a shift factors of various binders are plotted as a function of the temperature difference between the generic test temperature T and the reference temperature T_{ref}, selected in this study equal to 0 ℃. It can thus be observed that CNTs did not significantly affect the temperature dependency of the base bitumen when used in binary composites. On the contrary, the effect of polymer modification was evident in the range of high in-service temperatures and was found to be strictly dependent upon the molecular arrangement of the employed SBS. In fact, changes associated to the presence of a radial polymeric structure were higher than those corresponding to the existence of a linear polymeric structure and comparable to those obtained in the case of both BLC and BRC ternary blends.

In order to assess the temperature dependency of considered materials in quantitatively and synthetic terms, the shift factors determined with the LCPC method were used to calculate the so-called defining temperature T_d, following the procedure described by Christensen et al. [24]. As conceptually illustrated in Figure 3b, T_d is a binder characteristic parameter that indicates the transition point from the region where the viscoelastic

response obeys to the Arrhenius law to the region in which experimental data can be better described by the William-Landel-Ferry (WLF) model. The Arrhenius and WLF shift-factor functions, which are usually adopted in the low and in the intermediate-to-high range of in-service temperatures, respectively, are presented in Eq. 4-5:

$$log\left(a_{(T,T_d)}\right) = \frac{E_a}{2.303 \cdot R} \cdot \left(\frac{1}{T} - \frac{1}{T_d}\right); \quad for\ T < T_d \qquad \text{Eq. 4}$$

$$log\left(a_{(T,T_d)}\right) = \frac{-C_1 \cdot (T - T_d)}{C_2 + T - T_d}; \quad for\ T > T_d \qquad \text{Eq. 5}$$

where E_a is the activation energy, R is the ideal gas constant, while C_1 and C_2 are empirically determined coefficients.

Obtained results are presented in Table 7. The negligible decrease in the T_d value computed for binder BC with respect to B, confirms that the addition of CNTs did not significantly alter the temperature dependency of base bitumen. Such a result is coherent with the findings of other researchers [13], who reported that although CNTs have the potential to reduce temperature susceptibility of bitumen, relative variations are expected to be very low for CNT dosages of the order of 0.5 %. On the other hand, the use of the polymeric additives induced significant changes in the response of binary blends, with a more evident T_d variation recorded in the case of radial SBS. When considering ternary blends, it was found that while the addition of CNTs to BR did not provide any further significant effects, the addition of CNTs to BL induced changes that were higher than those observed for all other blends. This outcome suggests that in the case of the binder prepared with linear SBS, the nano-particles were more effective in interfering with the relaxation phenomena occurring in the binder matrix.

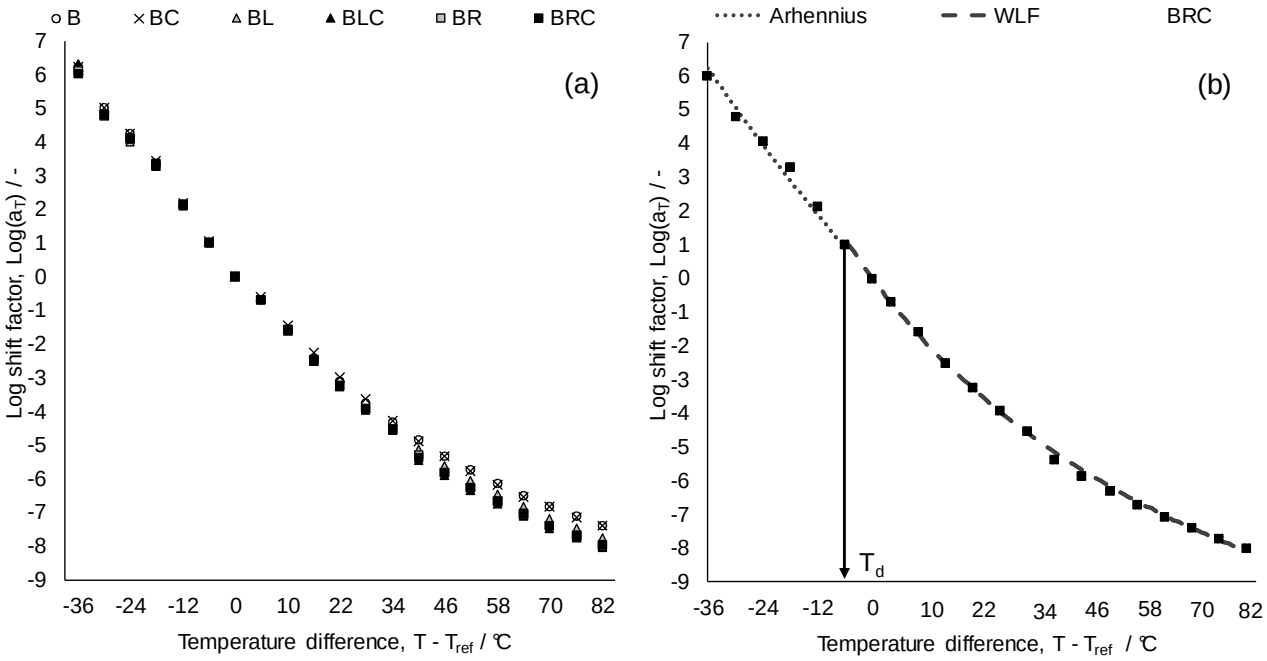

Figure 3. (a) Shift factors at a reference temperature of 0 ℃ (all binders); (b) T_d definition (binder BRC)

Table 7. Defining temperatures T_d.

	B	BC	BL	BR	BLC	BRC
T_d / ℃	-10.8	-10.9	-7.8	-6.1	-5.5	-6.2

4.3 Complex modulus

The viscoelastic behaviour of bituminous binders is usually presented in terms of $|G^*|$ and δ master curves, by means of which the evolution of material properties is described over a wide range of reduced loading frequencies ω_R. An example of master curves obtained for the BLC blend by making use of the shift factors determined with the LCPC method at the reference temperature of 0 ℃ is shown in Figure 4. Diagrams indicate that even in the most critical case of ternary blends, the use of the numerically derived shift factors yielded almost continuous curves.

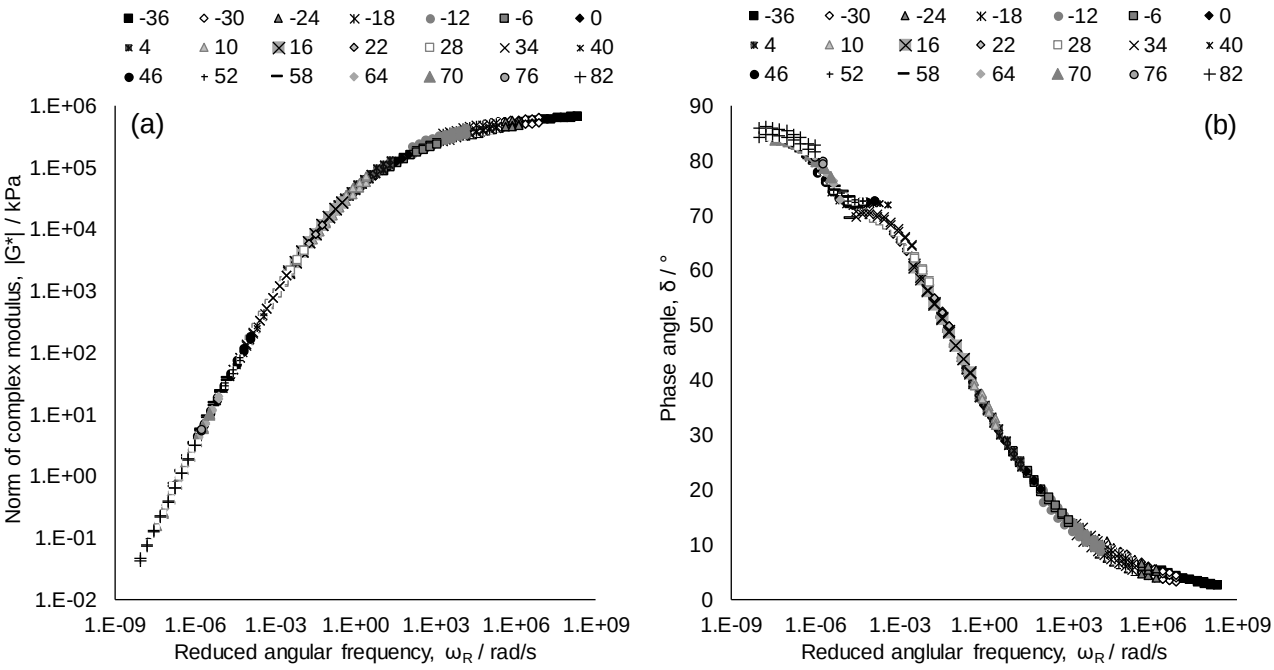

Figure 4. Master curves of the (a) norm and (b) phase angle of the complex modulus (binder BLC).

In order to seek quantitative relations between the rheological response of conventional binders and that of nano-structured composites, a linear viscoelastic modelling approach based on physical analogical elements was adopted. In particular, experimental data were fitted by making use of the continuous spectrum defined by the 2s2p1d model [25], considered more appropriate than discrete spectra for the description of complex rheological behaviour. As depicted in Figure 5, the 2s2p1d model is defined by the assemblage of 2 springs (2s), 2 parabolic creep elements (2p) and 1 dashpot (1d).

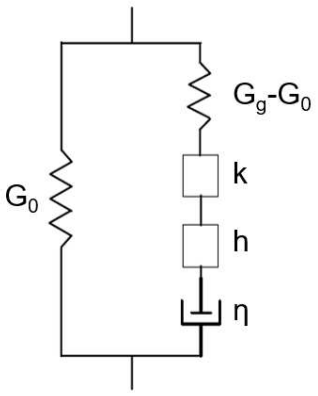

Figure 5. Representation of the 2s2p1d model.

As per the 2s2p1d model (Eq. 6), the complex modulus G^* at a given temperature is defined by seven constants (G_0, G_g, α, k, h, β, and τ_0, with $0 < k < h < 1$).

$$G^*(\omega) = G_0 + \frac{G_g - G_0}{1 + \alpha(i\omega\tau)^{-k} + (i\omega\tau)^{-h} + (i\omega\beta\tau)^{-1}} \quad \text{Eq. 6}$$

where characteristic time τ and Newtonian viscosity η are calculated by means of Eq. 7-8

$$\tau = a_T \cdot \tau_0 \quad \text{Eq. 7}$$

$$\eta = (G_g - G_0)\beta\tau \quad \text{Eq. 8}$$

In order to compute the norm and the phase angle of the complex modulus, the imaginary (Im) and the real (Re) parts of the complex modulus, that correspond to the loss modulus G'' and storage modulus G', respectively, need to be isolated from Eq. 6 as detailed in the following (Eq. 9-14):

$$G^*(\omega) = G_0 + \frac{(G_g - G_0) \cdot (A(\omega) - iB(\omega))}{A^2(\omega) + B^2(\omega)} \quad \text{Eq. 9}$$

$$G^*(\omega) = [Re] + i\,[Im] = \left[G_0 + \frac{(G_g - G_0) \cdot A(\omega)}{A^2(\omega) + B^2(\omega)}\right] + i\left[\frac{(G_g - G_0) \cdot (-B(\omega))}{A^2(\omega) + B^2(\omega)}\right] \quad \text{Eq. 10}$$

$$A(\omega) = 1 + \alpha(\omega\tau)^{-k} \cdot cos\left(\frac{k\pi}{2}\right) + (\omega\tau)^{-h} \cdot cos\left(\frac{h\pi}{2}\right) \quad \text{Eq. 11}$$

$$B(\omega) = -(\omega\beta\tau)^{-1} - \alpha(\omega\tau)^{-k} \cdot sin\left(\frac{k\pi}{2}\right) - (\omega\tau)^{-h} \cdot sin\left(\frac{h\pi}{2}\right) \quad \text{Eq. 12}$$

$$|G^*(\omega)| = \sqrt{[Re]^2 + [Im]^2} \quad \text{Eq. 13}$$

$$\delta = tan^{-1}\left(\frac{Im}{Re}\right) \quad \text{Eq. 14}$$

Due to the high degree of freedom of the model, its parameters were derived by using a trial-and-error method in combination with a solver tool until a good correspondence between experimental data and fitted curves was found in the Cole-Cole and Black plots, and in master curves of the norm and phase angle of the complex modulus [26]. Moreover, the static modulus G_0 and the glassy modulus G_g, which represent the moduli when the frequency approaches zero and infinite, respectively, were fixed at the beginning of the optimization process. Given that values of the static modulus for binders can be considered as negligible, G_0 was assumed to be equal to zero, thus reducing the model parameters to six. In the case of G_g, values were determined in a preliminary phase by modelling experimental data retrieved in the range comprised between -6 ℃ and -36 ℃. An example of experimental data a nd 2s2p1d curves for base bitumen B is displayed in Figures 6 and 7, where a graphical representation of the model parameters is also provided. 2s2p1d model parameters determined from regression analysis are summarized in Table 8.

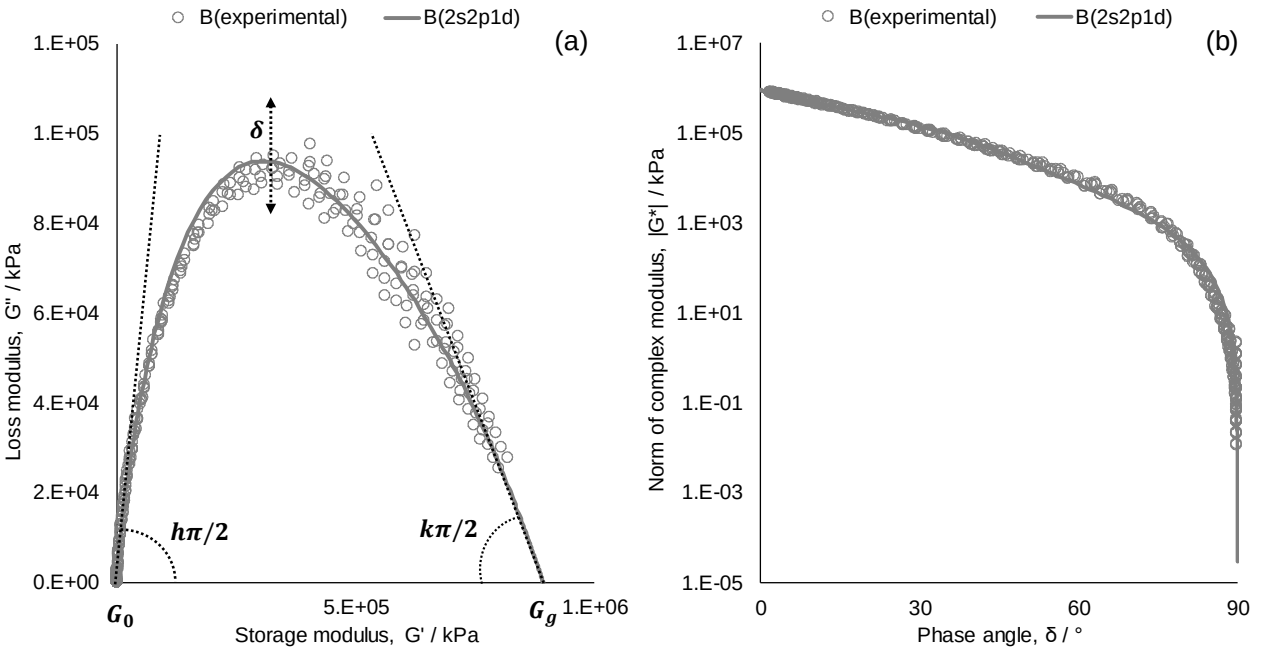

Figure 6. Cole-Cole (a) and Black (b) plots (binder B).

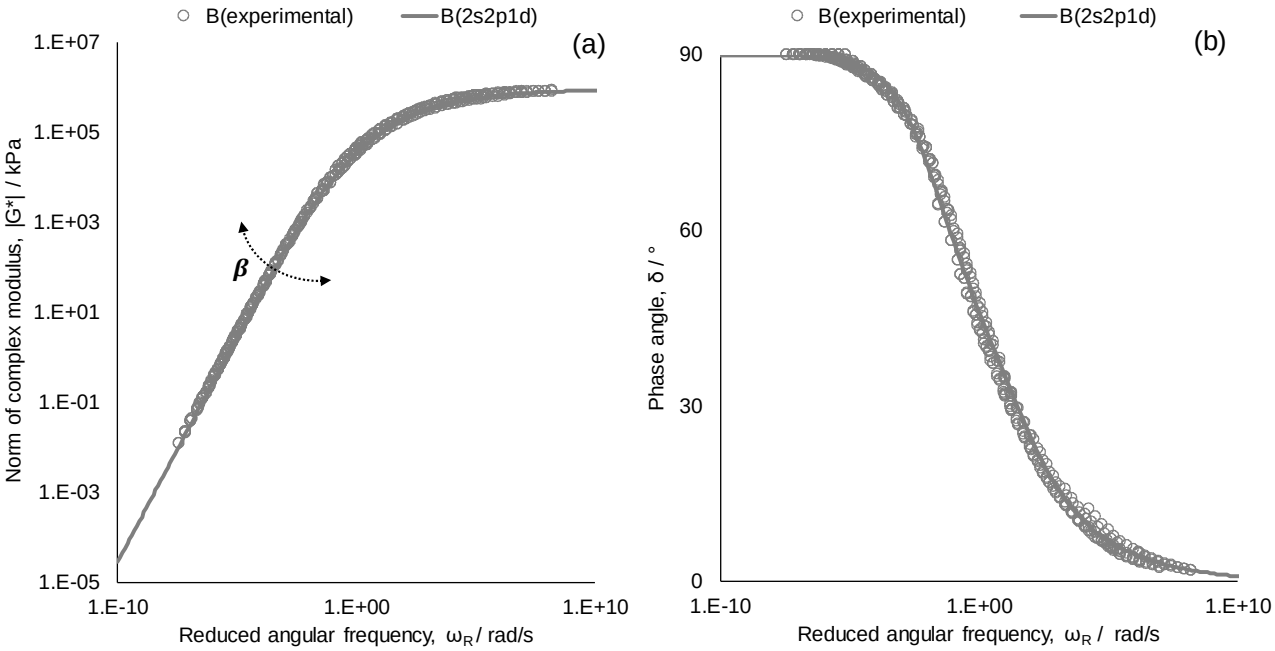

Figure 7. Norm (a) and phase angle (b) master curves (binder B).

Table 8. 2s2p1d model parameters.

	B	BC	BL	BR	BLC	BRC
G_0 / kPa	0	0	0	0	0	0
G_g / kPa	8.91E+05	8.13E+05	7.94E+05	7.94E+05	7.76E+05	7.59E+05
α	1.76	2.19	2.92	4.14	3.96	3.94
τ_0	0.45E-02	1.52E-02	1.77E-02	4.80E-02	3.67E-02	4.75E-02

β	71	36	127	154	163	208
h	0.55	0.63	0.63	0.68	0.66	0.70
k	0.20	0.23	0.21	0.23	0.22	0.34

The glassy modulus G_g, governed by the material properties in the low temperature (or high frequency) domain, was found to be marginally affected by the addition of CNTs and SBS polymers, with a slight tendency to decrease when progressively passing from the base bitumen to ternary blends.

On the contrary, the α parameter increased significantly with the addition to base bitumen of CNTs or SBS polymer, and a further increase was observed when combining CNTs and SBS to produce ternary composites. However, a distinction can be made between BLC and BRC blends that stems from the comparison of these blends to corresponding BL and BR binary systems. In fact, it was observed that BLC had a higher α value with respect to BL, thus revealing that an actual interaction takes place between CNTs and linear SBS. In the case of BR and BRC, values were similar to each other, indicating that the increase of the α parameter with respect to base bitumen is basically due to presence of radial SBS, with no effects produced by CNTs. Analogous considerations can be drawn from the analysis of τ_0 values. It is worth nothing that the α parameter controls the peak value of the loss modulus G'' in the low temperature (or high frequency) domain, while τ_0 governs the slope of the $|G^*|$ master curve in the range of high temperatures (or low frequencies).

A rise in β was also observed when comparing base bitumen to binary blends and these ones to ternary composites. The only exception was recorded in the case of blend BC for which, however, the lower value of β was balanced by the increment in τ_0, thus leading to an overall increase of the steady-state viscosity.

h and k exponents, which provide information on the slope of the Cole-Cole diagram at low and high values of the storage modulus, showed a slight increase when passing from base bitumen B to binary blends BC, BL, and BR as well as when passing from BL and BR binary blends to ternary nanocomposites containing CNTs.

On the basis of the discussion provided above, it can be stated that CNTs and linear SBS induced the lowest effects on the rheological behaviour of base bitumen when used individually. Moreover, when combined together, they led to significant mutual interactions which reflected on the overall rheological properties of the corresponding ternary composite. On the contrary, the response of the ternary blend containing radial SBS was mostly governed by the polymer, indicating the existence of a negligible interaction with the nano-sized component.

4.4 Apparent molecular weight distribution

Experimental results obtained from the rheological tests described in section 3 were analysed further in order to determine the molecular weight (MW) distribution of the various binders and ultimately derive information on their internal structure. Given the close relationship between the MW of materials and their viscoelastic properties [27], such a task has been addressed by several Authors who have adopted inverse mechanical approaches based on DMA data [28-31]. In such a context, it has been emphasized that the MW distribution of a bituminous binder is related to the characteristics of the crude oil from which it is derived, to the specific refinement process, and to the additives, if any, used to modify its properties [28].

By modelling bitumen as a continuity of molecular species, where each molecule relaxes at a specific frequency, it can be assumed that a generic molecular specie does not contribute to the mechanical response of the system under its specific relaxation frequency, condition at which it starts acting as a diluent for the unrelaxed molecules [28-31]. Coherently with such a descriptive model, for the various binders subjected to testing, the phase angle was hypothesized to be proportional to the fraction of relaxed molecules at a specific frequency [28]. Hence, the curve of the cumulative function of the molecular weight $Cumf(MW)$ was considered proportional to the phase angle master curve, as detailed in Eq. 15:

$$Cumf(MW) = A + B \cdot \delta(MW)$$ Eq. 15

where A and B are two constants determined from extreme ideal configurations of the MW. When the MW approaches zero the phase angle is equal to zero and $Cumf(MW)$ is also equal to zero: as a consequence, constant A is set equal to zero. When the MW approaches infinite, the phase angle is equal to $\pi/2$ and the $Cumf(MW)$ is therefore equal to 1: as a consequence, constant B is set equal to $2/\pi$.

By numerically differentiating Eq. 15 with phase angle data obtained from the 2s2p1d model, the molecular weight probability density $f(MW)$ can be computed at each molecular weight by means of Eq. 16:

$$f(MW) = \frac{dCumf(MW)}{dLog(MW)} \cong \frac{\Delta Cumf(MW)}{\Delta Log(MW)}$$ Eq. 16

Since the mechanical response of colloidal-like systems such as bitumen is assumed to be governed by molecular associations rather than molecules in the strict chemical sense, in the subsequent analyses reference was made to the apparent molecular weight (AMW), which also takes into account molecular arrangements caused by secondary bonds.

Apparent molecular weight distribution curves obtained as illustrated above for all binders are displayed in Figure 8a. In order to identify different molecular populations of which the binders are composed, deconvolution of the apparent molecular weight distribution was performed arbitrarily by considering three Gaussian functions, as illustrated in the example shown in Figure 8b. Deconvolution outputs are listed in Table 9, where for each Gaussian distribution the mean μ, the standard deviation σ and the percentage relative fraction are given.

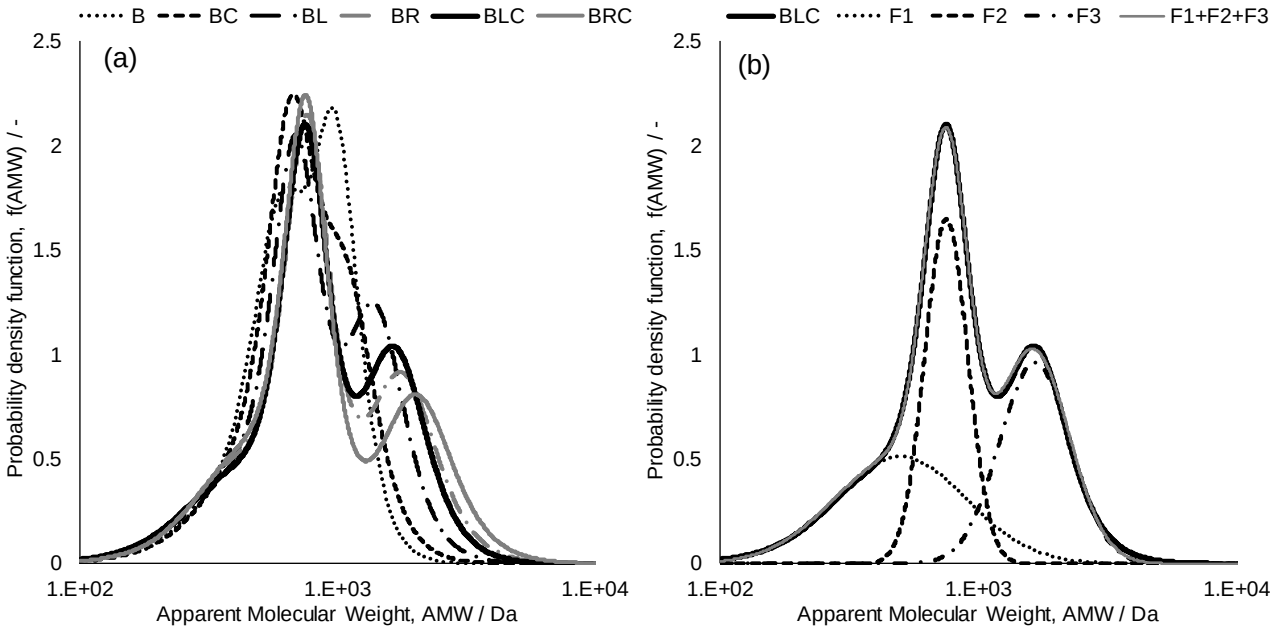

Figure 8. (a) Apparent molecular weight distribution curves; (b) Graphical representation of deconvolution (binder BLC).

Table 9. Deconvolution outputs: mean, standard deviation and relative percentage of molecular groups (F1, F2, and F3).

Apparent molecular group		B	BC	BL	BR	BLC	BRC
F1	$\mu_{Log(AMW / Da)}$	2.34	2.34	2.84	2.74	2.70	2.74
	$\sigma_{Log(AMW / Da)}$	0.13	0.16	0.30	0.26	0.25	0.25
	Relative fraction / %	3.9	5.5	50.6	39.0	32.7	39.9
F2	$\mu_{Log(AMW / Da)}$	2.85	2.81	2.84	2.89	2.88	2.88
	$\sigma_{Log(AMW / Da)}$	0.18	0.04	0.08	0.08	0.08	0.08
	Relative fraction / %	81.8	5.0	21.8	28.8	32.9	33.0

F3	$\mu_{Log(AMW\ /\ Da)}$	3.01	2.89	3.15	3.26	3.22	3.32
	$\sigma_{Log(AMW\ /\ Da)}$	0.06	0.20	0.10	0.14	0.14	0.15
	Relative fraction / %	14,3	89.5	27.6	32.2	34.4	27.1

When comparing bitumen B and blend BC to each other, it is interesting to observe that the presence of CNTs induced a perturbation in the colloidal order of the base bitumen. This can be noted from the overall shift towards lower apparent molecular weights found for BC, in which the fraction of the base bitumen characterized by the higher molecular weight (F3) underwent a certain structural breakdown.

The main effect caused by the presence of the SBS polymer in binary blends was the rise, with respect to the base bitumen, of a molecular group characterized by a higher apparent molecular weight. This is reflected by the mean values of the F3 molecular group that were around 1400 Da and 1800 Da for linear and radial SBS, respectively. Similarly, the addition of CNTs to polymer-modified blends induced a further shift towards higher mean apparent molecular weights with respect to the reference corresponding binary composites. Regardless of the mean apparent molecular weight achieved as a result of modification, it is noteworthy that the group with higher AMW in the case of linear SBS passed from 27.6 % to 34.4 %, while in the case of radial SBS it passed from 32.2 % to 27.1 %. Based on these outcomes it can be hypothesized that a major amount of complex structures aroused by combining CNTs and linear SBS, probably as a consequence of more stable and continuous interactions which occurred between these components.

5 Morphology

Rheological characterization of blends was complemented with fluorescence microscopy analysis, with the purpose of gathering qualitative information about the morphology of materials.

Morphological analysis was performed by making use of a Laborlux S fluorescence microscope from Leica, equipped with a EF 160/0.17 objective (40x magnification and 0.65 aperture) in conjunction with a digital camera. In this type of analysis, results may be affected by the specimen preparation technique due to the existence of potential artefacts created by manipulation of material. Based on indications drawn from literature, a “drop method” was used in this study since it is well suited to have a view of the morphology at the conditions where the sample is taken [32]. According to such a method, a drop of binder preheated at 150 ℃ was placed between glass slides and pressed into a thin film. Before visual inspections, specimens were left to cool at room temperature for a fixed time of 5 minutes.

In Figure 9 images are displayed only for the four blends containing the polymeric additive, since the neat and the CNT-modified binders do not exhibit any fluorescence property by nature.

Inspection of the morphological arrangements of composites prepared with the linear SBS additive revealed that CNTs affected the thermodynamic equilibrium of the two-phase system to a non-negligible extent. Although both blends showed a continuous polymeric phase, a higher homogeneity was achieved with CNTs, as indicated by the finer internal structure of binder BLC, in which smaller and more regular domains were observed in comparison to binder BL. This result suggests that CNTs can interact with swelling phenomena which take place in the SBS, promoting the migration of the light components of bitumen from the asphaltene-rich phase to the polymer-rich phase. It is worth to mention that this hypothesis is in good agreement with the strengthened interfacial interactions reported in other experimental studies on ternary nanocomposites carried out by combining laboratory experiments with molecular dynamic simulations [12,15].

In the case of blends prepared with the radial polymeric additive, it can be observed that the binary BR blend showed a homogeneous morphological arrangement characterized by a well-connected polymeric phase. On the other hand, the ternary BRC blend exhibited an inhomogeneous internal structure, where both roundish- and striped-shaped polymeric domains appeared clearly dispersed in the continuous bituminous matrix. While CNTs played the role of compatibility activators in the case of bitumen modification with linear SBS, in the case of radial SBS they seemed to intensify the thermodynamic instability of blends, thus

hindering the interphase anchorage between polymer and bitumen. Such results strongly support the outcomes derived from the rheological investigation described above.

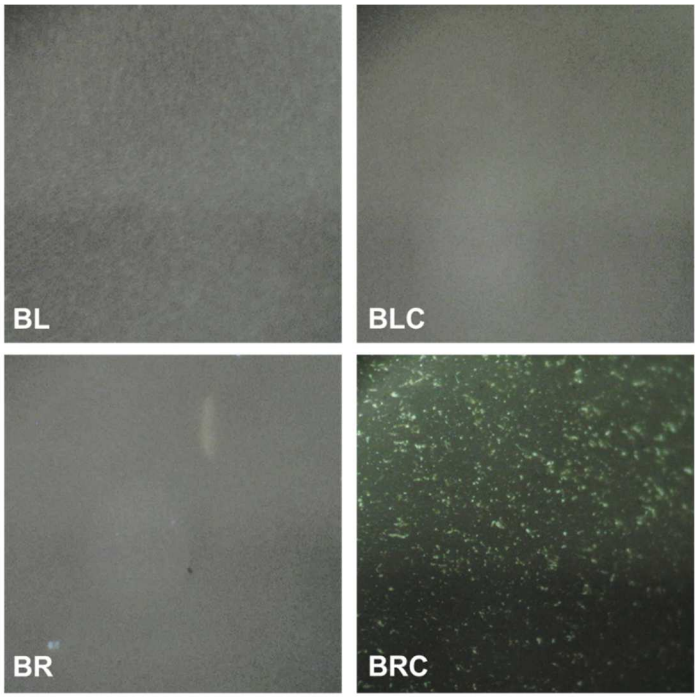

Figure 9. Morphology of binary and ternary polymer-modified binders.

6 CONCLUSIONS

Results presented in this paper indicate that the molecular structure of SBS employed as bitumen modifier strongly affects the final properties of ternary bituminous-based nanocomposites containing non-functionalized multiwall CNTs.

Specifically, polymer architecture was found to play a crucial role in promoting effective interactions with the CNTs. This is evident from the diverging outcomes emerged from the rheological characterization and was confirmed by the morphological analyses. In the case of linear SBS, CNTs acted as compatibility activators, leading to the formation of more stable and continuous interactions between the bituminous matrix and the polymeric phase. In the case of radial SBS, CNTs intensified the thermodynamic instability of ternary systems, thus jeopardizing the beneficial effects provided by modification.

In order to support the findings of this study, laboratory investigations should be extended to a wider array of base materials and possible combinations among them. Moreover, the effects of the blending protocol employed for material preparation need to be evaluated further. The analysis of rheological properties in the non-linear domain also deserves consideration in future research.

Acknowledgments The study reported in this paper is part of the FIRB research project on “Innovative nano-structured and polymer-modified bituminous materials” funded by the Italian Ministry of Education, University and Research (MIUR) (Grant RBFR10JOWO). Support of Bitumtech s.r.l. for morphological analyses is gratefully acknowledged.

Data statement The raw/processed data required to reproduce these findings cannot be shared at this time as the data also forms part of an ongoing study.

REFERENCES

[1] Zhu J, Birgisson B, Kringos N. Polymer modification of bitumen: Advances and challenges. European Polymer Journal 54 (2014), pp. 18-38.

[2] Polacco G, Filippi S, Merusi F, Stastna G. A review of the fundamentals of polymer-modified asphalts: Asphalt/polymer interactions and principles of compatibility. Advances in Colloid and Interface Science 224 (2015), pp. 72-112.

[3] Polacco G, Stastna J, Biondi D, Zanzotto L. Relation between polymer architecture and nonlinear viscoelastic behavior of modified asphalts. Current Opinion in Colloid & Interfacial Science 11 (2006), pp. 230-245.

[4] Polacco G, Muscente A, Biondi D, Santini S. Effect of composition on the properties of SEBS modified asphalts. European Polymer Journal 42 (2006), pp. 1113-1121.

[5] Schaur A, Unterberger S, Lackner R. Impact of molecular structure of SBS on thermomechanical properties of polymer modified bitumen. European Polymer Journal 96 (2017), pp. 256-265.

[6] Gopalakrishnan K, Birgisson B, Taylor P, Attoh-Okine N. Nanotechnology in civil infrastructures: a paradigm shift. Springer, Berlin, 2011.

[7] Li R, Xiao F, Amirkhanian S, You Z, Huang J. Developments of nano materials and technologies on asphalt materials – A review. Construction and Building Materials 143 (2017), pp. 633-648.

[8] Santagata E, Baglieri O, Tsantilis L, Chiappinelli G. Storage stability of bituminous binders reinforced with nano-additives. In: 8th RILEM International Symposium on Testing and Characterization of Sustainable and Innovative Bituminous Materials. Ancona: Springer (2015) pp. 75-87.

[9] Santagata E, Baglieri O, Tsantilis L, Chiappinelli G. Effect of sonication on the high temperature properties of bituminous binders reinforced with nano-additives. Construction and Building Materials 75 (2015), pp. 395-403.

[10] Santagata E, Baglieri O, Tsantilis L, Chiappinelli G, Dalmazzo D. Fatigue and healing properties of bituminous mastics reinforced with nano-sized additives. Mechanics of Time-Dependent Materials 20 (2016), pp. 367 387.

[11] Dresselhaus MS, Dresselhaus G, Avouris Ph. Carbon nanotubes: Synthesis, Structure, Properties, and Applications. Topics in Appl Phys 80. Springer, New York, 2001

[12] Wang P, Zhai F, Dong Z, Wang L, Liao J, Li G. Micromorphology of asphalt modified by polymer and carbon nanotubes through molecular dynamics simulation and experiments: Role of strengthened interfacial interactions. Energy & Fuels 32 (2018), pp. 1179-1187.

[13] Goli A, Ziari H, Amini A. Influence of carbon nanotubes on performance properties and storage stability of SBS modified asphalt binders. Journal of Materials in Civil Engineering 29:8 (2017), DOI: 10.1061/(ASCE)MT.1943-5533.0001910

[14] Wang P, Dong Z-J, Tan Y-Q, Liu Z-Y. Effect of multiwall carbon nanotubes on the performance of styrene-butadiene-styrene copolymer modified asphalt. Materials and Structures 50:17 (2017).

[15] Shu B, Wu S, Pang L, Javilla B. The utilization of multiple-wall carbon nanotubes in polymer modified bitumen. Materials 10:4 (2017), DOI: 10.3390/ma10040416

[16] Santagata E, Baglieri O, Dalmazzo D, Tsantilis L. Rheological and chemical investigation on the damage and healing properties of bituminous binders. J Assoc Asph Paving Technol 78 (2009), pp. 567-595

[17] Holleran, G, Holleran, H. Bitumen Chemistry Using Cheaper Sources: An Improved Method of Measurement by TLC-FID and the Characterisation of Bitumen by Rheological and Compositional Means. In 24th ARRB Conference, 34. Australian Road Research Board. Melbourne, Victoria, 2010.

[18] Santagata E, Baglieri O, Tsantilis L, Chiappinelli G. Fatigue properties of bituminous binders reinforced with carbon nanotubes. International Journal of Pavement Engineering 16 (2015), pp. 80-90.

[19] Santagata E, Baglieri O, Tsantilis L, Chiappinelli G, Dalmazzo D. Bituminous-based nanocomposites with improved high-temperature properties. Composite Part B: Engineering 99 (2016), pp. 9-16.

[20] Santagata E, Baglieri O, Tsantilis L, Chiappinelli G. Fatigue and healing properties of nano-reinforced bituminous binders. International Journal of Fatigue 80 (2015), pp. 30-39.

[21] Airey GD. Use of black diagrams to identify inconsistencies in rheological data. Road Mater. and Pavement Des. 3:4 (2002) pp. 403-424.

[22] Yusoff NI Md, Chailleux E, Gordon AD. A comparative study of the influence of shift factors equations on master curve construction. International Journal of pavement research and technology 4:6 (2011), pp. 324-336.

[23] Chailleux Emmanuel, Ramond Guy, Such Christian, de La Roche Chantal. A mathematical-based master-curve construction method applied to complex modulus of bituminous materials. Road Materials and Pavement Design. EATA (2006), pp. 75-92.

[24] Christensen DW, Anderson DA. Interpretation of dynamic mechanical test data for paving grade asphalt cements. Journal of the Association of Asphalt Paving Technologists 61 (1992), pp. 67-116.

[25] Olard F, Di Benedetto H. General “2S2P1D” model and relation between the linear viscoelastic behaviours of bituminous binders and mixes. Road Materials and Pavement Design 4:2 (2003), pp.185-224.

[26] Yusoff NI Md, Damien M, Ginoux MS, Rosli H M, Gordon AD., Di Benedetto H. Modelling the rheological properties of bituminous binders using the 2s2p1d model. Construction and Buiding Materials 38 (2013), pp. 395-406.

[27] Ferry JD. Viscoelastic properties of polymers. 1980, 3rd ed. New York, NY: John Wiley.

[28] Themeli A, Chailleux E, Farcas F, Chazallon C, Migault B. Molecular weight distribution of asphaltic paving binders from phase-angle measurements. Road Materials and Pavement Design 16:S1 (2015), pp. 228-244.

[29] Tuminello WH. Molecular weight and molecular weight distribution from dynamic measurements of polymer melts. Polymer Engineering & Science 26 (1986), pp. 1339–1347.

[30] Zanzotto L, Stastna J, Ho S. Molecular weight distribution of regular asphalts from dynamic material functions. Materials and Structures 32 (1999), pp. 224-229.

[31] Krolkral K, Haddadi S, Chailleux E. Quantification of asphalt binder ageing from apparent molecular weight distributions using a new approximated analytical approach of the phase angle. Road Materials and Pavement Design (2018), DOI:10.1080/14680629.2018.1536610.

[32] Soenen H, Lu X, Redelius P. The morphology of bitumen-SBS blends by UV microscopy: An evaluation of preparation methods. Road Materials and Pavement Design 9:1 (2008), pp. 97-110.